High order QCD predictions of the Higgs boson production cross-section at the LHC

Achilleas Lazopoulos, Stephan Bühler

1 Introduction

The LHC is marching through its third year of operation and the first tantalizing hits for a Higgs boson have already appeared. The corresponding experimental analyses rely crucially on theory predictions for the number of Higgs events expected within the Standard Model (SM) or theories beyond it that contain one or more Higgs bosons.

The number of Higgs events expected from each channel is currently evaluated in an involved way. the overall normalization is retrieved from very precise higher order inclusive calculations that have reached the level of next-to-next-to-leading order (NNLO) in the QCD and next-to-leading order (NLO) in the electroweak coupling for all production processes of immediate interest for the LHC discovery phase. Kinematic distributions are, on the other hand, predicted with the help of parton showers matched with hard matrix elements at the LO or NLO level. The distributions thus produced have been cross-checked against fixed order NNLO differential computations for the case of the (dominant) gluon fusion production mode. When such NNLO computations are available, they can be used to compare directly with distributions from experimental data under the assumption that showering and hadronization effects are negligible so that the parton level description of the fixed order calculation is a good approximation.

In what follows the focus will be on Higgs production cross-sections for the LHC and the precision with which we know them as of the time of writing of this proceeding.

2 Associated production and vector boson fusion

The associated production mechanism is not as prominent at the LHC as it has been at Tevatron and until recently it was not considered a viable discovery channel. The situation has changed thanks to various insightful proposals on how to improve the signal to background ratio, and the channel is now contributing to exclusion or discovery combinations for both full-range LHC experiments. The focus is on configurations with kinematically boosted Higgs bosons decaying to a pair of bottom quarks. The inclusive production rate is known at NNLO [?]. The NLO EW corrections are also known [?]. The perturbative expansion is very stable leading to K-factors of 1.27 at NLO and 1.28 at NNLO, similarly to what happens in Drell-Yan. The uncertainty due to factorization and renormalization scales is reduced to $\sim 3\%$. Recently the fully differential NNLO calculation was completed [?] including the LO decay to bottom pairs which allows for studies in the boosted region of interest. First phenomenological studies show that, as in the case of gluon

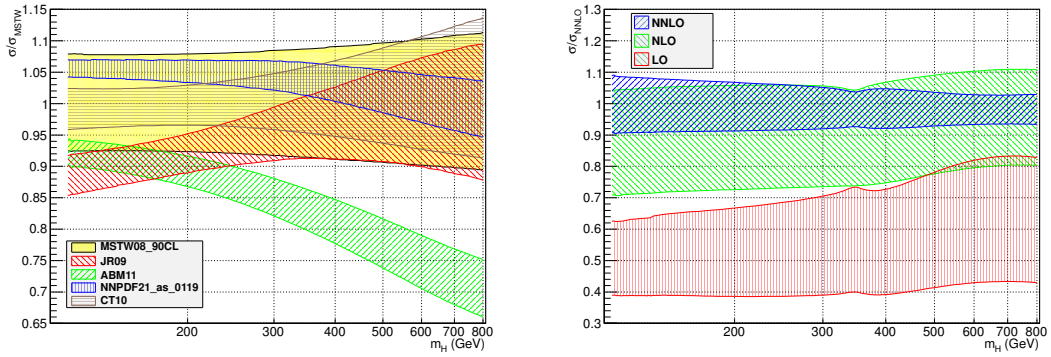

Figure 1: Higgs in gluon fusion. Left: production cross sections with various PDF sets and their uncertainty bands, normalized to the cross section calculated with the central MSTW08 grid. Note that the MSTW08 uncertainty band is at 95%CL and that the bands for NNPDF and CT10 do **not** include the induced error due to α_s variation. Right: Scale uncertainty per QCD order in the interval $\mu_f = \mu_r = \mu \in [m_H/4, m_H]$.

fusion, the presence of aggressive kinematical cuts can alter significantly the acceptance rates at the LHC. We have recently completed [?] the fully differential decay $H \to b\bar{b}$ which will be soon interfaced with the production computation.

The vector boson fusion channel is of particular interest since it is an indirect probe of vector boson scattering. Its production cross section is known to NLO QCD[?] as well as NLO EW [?]. The DIS-like component of the NNLO calculation is also known [?] and the perturbative convergence is excellent, as demonstrated at fig.4.1 of the work by Bolzoni et al. [?].

3 Gluon fusion $gg \to H$

This is the dominant production mode at the LHC and the one that has been studied most extensively. The NNLO QCD corrections are know already for a decade now, in the heavy quark effective theory (HQET) approximation [?,?,?] which has recently been shown [?,?] to be an excellent approximation. At the NLO level the production rate is known exactly (i.e. including finite top and bottom mass effects as well as their interference). Electroweak corrections at the two-loop level [?,?,?] and mixed QCD electroweak corrections [?,?] are also known. Threshold [?] and soft gluon [?] re-summation have also been performed to the NNLL level and the soft terms of the NNNLO have been calculated [?]. We have recently implemented [?] all known fixed order contributions up to NNLO in a new publicly available program for the inclusive cross-section at hadron colliders, `ihixs`. We have added to the existing literature the possibility to account for finite top width effects in the calculation, which were found to be negligible below the top threshold and only of the order of $\sim 2.5\%$ around the threshold and $\sim 1\%$ for a heavy Higgs. Moreover, `ihixs` delivers predictions for an arbitrary number of SM-like quarks and arbitrary rescalings of their Yukawa couplings. This allows for BSM predictions, an example of which is the cross section for an extended SM with four quark generations [?].

The SM cross-section predictions we recommend for the LHC at 8TeV have been published recently [?] and include uncertainties due to the factorization and renormalization scales, as well as the imprecise knowledge of the parton distribution functions.

3.1 PDF uncertainties

An impressive progress has been achieved in recent years towards increasing the precision and the reliability of parton density functions (PDF). There are currently five PDF providers using different data sets, theoretical assumptions, parameterizations and fitting techniques to predict

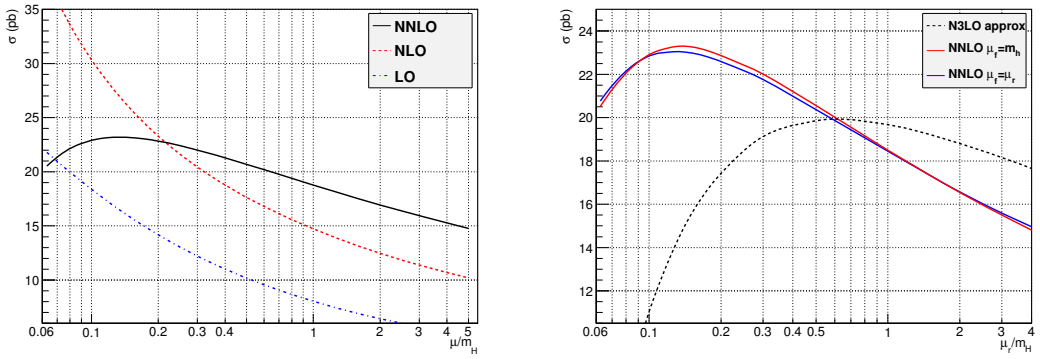

Figure 2: Higgs in gluon fusion: cross-section as a function of the ratio μ/m_H of the scale over the Higgs mass for fixed order (left) and the gluon fusion channel alone in NNLO with $\mu_r = m_H$, NNLO with $\mu_r = \mu_f = \mu$, and the NNNLO approximate soft terms from ref.24 (right).

the parton densities, that have already reached the NNLO level of accuracy. The resulting central values and uncertainty bands [a] for MSTW08, NNPDF, ABM11, JR09, as well as the recently released CT10NNLO PDFs, normalized to the central value for MSTW08, are shown in fig. **??**. It is seen that all "global" PDF sets agree within their uncertainties, while the ABM set clearly disagrees for all Higgs masses, with the discrepancy increasing with the Higgs mass. The difference can be partly attributed to the lower value for α_s used by the ABM collaboration (the value is an outcome of their fitting procedure and not an input parameter) but comparison to the NNPDF set adopting the lowest available value for α_s shows that there are further differences of a systematic nature. The issue should be resolved shortly, as predictions for SM processes using the different PDF sets will be compared with the LHC measurements with increasingly diminishing experimental uncertainty. Until then we find it prudent to provide cross section rates with the ABM11 set as our second benchmark set.

3.2 Scale uncertainty

Another important source of uncertainty comes from the arbitrary choice of renormalization and factorization scales used in the calculation. This uncertainty would vanish in an all orders computation and is therefore an artifact of the truncation of the perturbative series. It is usually taken as an indication of the size of the remaining, unknown, higher order corrections, beyond NNLO in the case of gluon fusion. However, such an estimate includes a certain degree of arbitrariness, as the choice of both the central scale used and the interval in which the scale is varied are only dictated by past experience and tradition.

In fig. **??** we show the cross section at LO, NLO, NNLO as a function of the scale μ. For the fixed order predictions up to NNLO, we keep the two scales equal, $\mu_f = \mu_r$ but it should be kept in mind that the dependence of the fixed order result on μ_f is very mild. This is reflected in fig. **??**(right) where the gluon fusion channel of the NNLO cross section in the EFT approximation for $\mu_f = m_H$ as a function of μ_r/m_H is shown and it is seen to almost completely overlap with the $\mu_f = \mu_r = \mu$ prediction. In fig. **??** we compare the fixed order result with the NNNLO approximate soft contributions [?].

Our choice of the central scale is $\mu = \mu_f = \mu_r = m_H/2$. This leads to a scale uncertainty per fixed order shown in fig. **??**. The motivation for choosing the central scale at $m_H/2$ comes from considerations on the convergence of the perturbative expansion:

[a] Note however that the MSTW08 uncertainty band reflects the 90%CL while for all other PDF sets it's at the 68%CL, and that the NNPDF and CT10 uncertainty bands do **not** include the uncertainty induced by α_s variation.

- We find it unnatural to separate μ_f from μ_r, thus inducing a further artificial dependence on $\log(\mu_f/\mu_r)$ that would vanish in an all orders result.

- Typical emission of extra partons happen at a scale $m_H/2$ or below and the average transverse momentum of the Higgs is between $m_H/4$ and $m_H/2$ for all Higgs masses. This indicates that a reasonable scale is $m_H/2$.

- At NLO the logarithmic dependence on μ is through the ratio $\log\left(\frac{\mu}{m_H(1-z)}\right)$ where z parametrizes the distance from threshold production. Choosing a scale equal or higher than the Higgs mass artificially enhances the contribution of this logarithm, as it was already noticed a decade ago [?].

- As shown in fig. **??** the convergence of the perturbative series in the low μ region is improved. That is reflected in the fact that the NLO scale uncertainty band fully engulfs the NNLO band.

- The NNNLO soft contributions, shown for the gg initial state channel in fig. **??**, whose variation lies within the NNLO scale uncertainty band when the scale is chosen low, lead to a similar conclusion.

Moreover, comparison with the NNLO prediction with threshold re-summation shows that it agrees below the per cent level with the fixed order result when $\mu = m_H/2$ and below and starts deviating from it for $\mu > m_H/2$. We have checked that the relative deviation of the threshold re-summation calculation and the fixed order one remains at the per mille level for all collider energies up to 20TeV, while for $\mu = m_H$ the two results differ by 5% or more at the entire energy range up to 20TeV.

3.3 High Higgs mass

If the Higgs boson is light, i.e. its mass is smaller than ~ 300 GeV, its line shape, measured as the invariant mass distribution of its decay products, is an uneventful spike well thinner than the corresponding experimental resolution in both the diphoton and the four leptons decay channel. If, on the contrary, the mass of the Higgs boson lies in the near TeV scale (i.e. if $m_H > 800$GeV) the width becomes comparable to its mass and the customary factorization of cross-sections in production and decay phases is not valid any more. Two related features call for our attention: (a) the zero width approximation used for low masses is not a valid approximation any more. Hence the off-shell contributions of the Higgs boson have to be included and the exact treatment of the Higgs propagator becomes a delicate issue in which Dyson resummation and gauge invariance have to be combined in a consistent way. (b) Signal-background (SB) interference with background diagrams cannot be ignored any more, especially in the experimentally interesting vector boson decay channels. In particular, as the mass of the Higgs approaches the TeV range, the cancellations between diagrams involving the Higgs boson and diagrams involving the longitudinal mode of the vector bosons, which ensure the unitarization of vector boson scattering, become stronger. Therefore ignoring the latter is no longer possible.

Using `ihixs` we have shown [?] that the treatment of the propagator has a severe impact on the line shape and the total cross section. An attempt to quantify the SB interference effects, using a prescription for the propagator based on the re-summation of $VV \to VV$ scattering amplitudes [?] (with the dominant contributions from both resonant and non-resonant Feynman diagrams) at the high energy regime shows that the distortions on both line shape and cross-section are too large to ignore for $m_H \geq 400$GeV. Studies of the impact of different propagator prescriptions on exclusion plots [?] show that including the emulated SB interference effects through the above

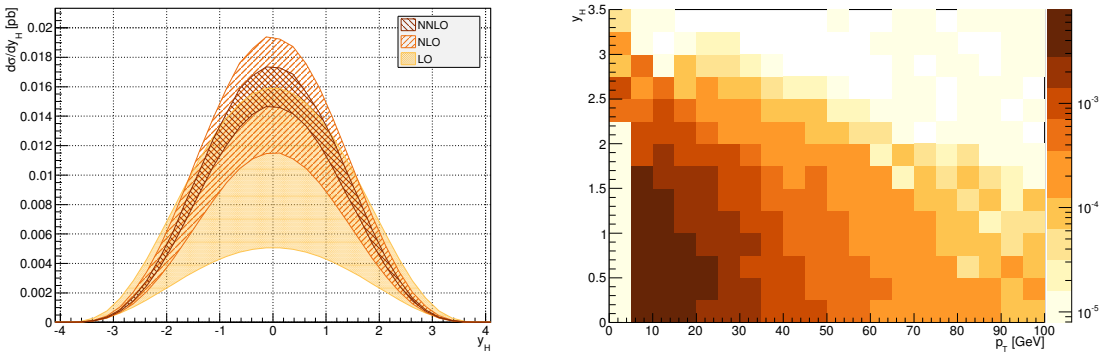

Figure 3: Higgs from bottom quark annihilation: Higgs rapidity distribution per QCD order with scale uncertainty bands (left) and doubly differential distribution in rapidity and transverse momentum(right).

prescription [?] as part of the signal hypothesis would lead to differences in exclusion limits for masses higher than 600GeV.

For these reasons we have refrained [?] from providing NNLO predictions for the Higgs production cross section for $m_H > 400$GeV. We believe that for Higgs bosons heavier than that, the SB interference, known at LO [?,?,?] should be included in the cross-section prediction and the corresponding LO uncertainty should be assigned to it. Since the NNLO K-factor for the signal diagrams alone is known to be ~ 2, one would in practice prefer to assign a SB related uncertainty to the full NNLO cross-section based on LO information, but it should be clear that this would be based on unwarranted assumptions on the magnitude of the NLO and NNLO SB diagrams.

4 Bottom quark annihilation: $b\bar{b} \to H$

In new physics models where the Higgs sector is non-minimal, the Yukawa coupling to bottom quarks is enhanced by a potentially large factor and the bottom quark annihilation becomes competitive to gluon fusion as a Higgs production mode. Moreover it is experimentally indistinguishable from gluon fusion and therefore its production rates add to those of the gluon fusion channel. The inclusive cross-section of the process is known to NNLO in QCD [?] as well as at NLO EW [?]. We have recently completed the fully differential NNLO calculation [?]. The rapidity distribution for the Higgs boson and its uncertainty band due to the factorization scale choice shows that the perturbative expansion in this channel is, as expected, smooth, see fig. **??**. In fig. **??** we can also see the doubly differential distribution over the rapidity and the transverse momentum of the Higgs boson. We have further implemented the diphoton decay channel and produced distributions in the presence of realistic experimental cuts, which demonstrates the fully differential nature of our calculation.

5 Conclusions

The inclusive cross-sections for Higgs production at the LHC have in general been studied extensively and are therefore known to relatively high precision. However there are several salient features in Higgs production via gluon fusion that deserve further attention and are currently the focus of theoretical investigations. In this short proceeding we point to some of those features, in anticipation of further developments.

References

1. O. Brein, A. Djouadi and R. Harlander, Phys. Lett. B **579** (2004) 149 [hep-ph/0307206].
2. M. L. Ciccolini, S. Dittmaier and M. Kramer, Phys. Rev. D **68** (2003) 073003
3. M. Ciccolini, A. Denner and S. Dittmaier, Phys. Rev. Lett. **99** (2007) 161803
4. M. Ciccolini, A. Denner and S. Dittmaier, Phys. Rev. D **77** (2008) 013002
5. P. Bolzoni, F. Maltoni, S. -O. Moch and M. Zaro, Phys. Rev. Lett. **105** (2010) 011801
6. P. Bolzoni, F. Maltoni, S. -O. Moch and M. Zaro, Phys. Rev. D **85** (2012) 035002
7. G. Ferrera, M. Grazzini and F. Tramontano, Phys. Rev. Lett. **107** (2011) 152003
8. C. Anastasiou, F. Herzog and A. Lazopoulos, JHEP **1203** (2012) 035
9. R. V. Harlander and W. B. Kilgore, Phys. Rev. Lett. **88**, 201801 (2002)
10. C. Anastasiou and K. Melnikov, Nucl. Phys. B **646**, 220 (2002)
11. V. Ravindran, J. Smith and W. L. van Neerven, Nucl. Phys. B **665**, 325 (2003)
12. R. V. Harlander and K. J. Ozeren, JHEP **0911** (2009) 088
13. A. Pak, M. Rogal and M. Steinhauser, JHEP **1002** (2010) 025
14. S. Actis, G. Passarino, C. Sturm and S. Uccirati, Nucl. Phys. B **811**, 182 (2009)
15. S. Actis, G. Passarino, C. Sturm and S. Uccirati, Phys. Lett. B **670**, 12 (2008)
16. U. Aglietti, R. Bonciani, G. Degrassi and A. Vicini, Phys. Lett. B **595**, 432 (2004)
17. W. Y. Keung and F. J. Petriello, Phys. Rev. D **80**, 013007 (2009)
18. C. Anastasiou, R. Boughezal and F. Petriello, JHEP **0904**, 003 (2009)
19. S. Catani, D. de Florian, M. Grazzini and P. Nason, JHEP **0307** (2003) 028
20. D. de Florian and M. Grazzini, Phys. Rev. Lett. **85** (2000) 4678
21. C. Anastasiou, S. Buehler, F. Herzog and A. Lazopoulos, JHEP **1112** (2011) 058
22. C. Anastasiou, S. Buehler, F. Herzog and A. Lazopoulos, JHEP **1204** (2012) 004
23. C. Anastasiou, S. Buehler, E. Furlan, F. Herzog and A. Lazopoulos, Phys. Lett. B **702** (2011) 224
24. S. Moch and A. Vogt, Phys. Lett. B **631** (2005) 48
25. M. H. Seymour, Phys. Lett. B **354** (1995) 409
26. A. Aeberli, F. Dulat and B. Mistlberger, Master Thesis
27. E. W. N. Glover and J. J. van der Bij, Phys. Lett. B **219** (1989) 488.
28. T. Binoth, M. Ciccolini, N. Kauer and M. Kramer, JHEP **0612** (2006) 046
29. J. M. Campbell, R. K. Ellis and C. Williams, JHEP **1110** (2011) 005
30. R. V. Harlander, W. B. Kilgore, Phys. Rev. **D68** (2003) 013001.
31. S. Dittmaier, M. Kramer, 1, A. Muck and T. Schluter, JHEP **0703** (2007) 114
32. S. Buehler, F. Herzog, A. Lazopoulos and R. Mueller, arXiv:1204.4415 [hep-ph].